

Effective temperature of active matter

Davide Loi,¹ Stefano Mossa,¹ and Leticia F. Cugliandolo²

¹ European Synchrotron Radiation Facility, BP 220, F-38043 Grenoble France

²Université Pierre et Marie Curie – Paris VI, LPTHE UMR 7589, 4 Place Jussieu, 75252 Paris Cedex 05, France

(Dated: February 2, 2008)

We follow the dynamics of an ensemble of interacting self-propelled particles in contact with an equilibrated thermal bath. We find that the fluctuation-dissipation relation allows for the definition of an effective temperature that is compatible with the results obtained using a tracer particle as a thermometer. The effective temperature takes a higher value than the temperature of the bath when the effect of the motors is not correlated with the structural rearrangements they induce. Instead, it takes a slightly lower value than the environmental temperature when susceptible motors are used.

Active matter is driven out of equilibrium by internal or external energy sources. Its constituents absorb energy from their environment or from internal fuel tanks and dissipate it by carrying out internal movements that lead to translational or rotational motion. A typical example is given by the eukaryotic cell cytoskeleton network [1] that is made of long polar filaments with attached motors. The latter exert stresses which deform the former and regulate the network dynamics. These structures exhibit a rich variety of viscoelastic properties; by rearranging their structure they change from plastic/fluid to elastic/solid phases and *vice versa*. Another celebrated example of active matter are self-propelled particle assemblies in bacterial colonies [2].

In this Letter we address the following fundamental question: which thermodynamic concepts, if any, can be applied to active matter? We focus on the definition of an *effective temperature*, T_{eff} , through the comparison of induced and spontaneous dynamic fluctuations [3]. The notion of such a T_{eff} was introduced in the study of (passive) glassy systems, that is to say, macroscopic objects with a sluggish relaxation that takes them to an asymptotic small-entropy production regime which is, though, still far from equilibrium. In these systems T_{eff} is a good thermodynamic concept. It admits a microcanonical-like definition in which only asymptotically dynamically accessible states contribute to the entropy [4]. T_{eff} can be measured by a fine-tuned thermometer, it satisfies a zeroth law in the sense that it takes the same value for all observables evolving in the same time-scale, and heat flows in the direction of negative effective temperature differences [3]. Moreover, it appears in the modification of fluctuation theorems when applied to systems that cannot equilibrate when let freely evolve [5]. These features were confirmed with numerical simulations of a variety of realistic glassy models [6] and a number of groups are testing these ideas experimentally on colloidal suspensions [7]. Theory suggests that the effective temperature should also be well-behaved in weakly driven systems – in a small entropy production regime [3]. This fact was put to the test in gently sheared super-cooled liquids and glasses [8], vibrated granular matter [4], and moving vor-

tex phases in superconductors [9]. In biologically inspired problems the relevance of T_{eff} was already stressed in studies of gene networks [10] and to reveal the active process in hair bundles [11].

The role played by T_{eff} in the stability of dynamic phases of motorized particle systems was stressed by Shen and Wolynes [12] with a variational analysis of the master equation of a similar model to the one we study here. In order to investigate the existence and properties of T_{eff} in active matter we study a schematic statistical physical model: a system of $i = 1, \dots, N$ massive, interacting and motorized spherical particles confined to a fixed volume, V , in 3d. Spherical particles are indeed too simple for real applications in the context of cytoskeleton studies but we choose them to highlight the effect of the non-equilibrium drive. Similar behaviour is expected for other geometries of the constituents. Particles are in contact with a thermal environment that is described by a random noise and a viscous drag. The particles' velocities \mathbf{v}_i thus evolve with the Langevin equation:

$$m_i \dot{\mathbf{v}}_i = -\xi m_i \mathbf{v}_i + \mathbf{f}_i^s + \mathbf{f}_i^M + \eta_i . \quad (1)$$

Here, $-\xi m_i \mathbf{v}_i$ is the frictional force and ξ the friction coefficient. η_i is a Gaussian white noise representing thermal agitation with zero mean, and correlations $\langle \eta_i(t) \eta_i(t') \rangle = 2\xi m_i T \delta(t - t')$ (we set $k_B = 1$ henceforth). The systematic mechanical conservative force on particle i due to all others is $\mathbf{f}_i^s \equiv \sum_{j=1}^N \mathbf{f}_{ij}^s = -\sum_{j=1}^N \nabla_i U(r_{ij})$ with the 2n-n Lennard-Jones potential [13] $U(r_{ij}) = 4\epsilon[(\sigma/r_{ij})^{2n} - (\sigma/r_{ij})^n]$. r_{ij} is the interparticle distance. The short-range repulsion, parametrized by σ , prevents the overlapping of the particles and it is then a (soft) measure of the particle diameter. The energy parameter, ϵ , describes the depth of the attraction. The mid-range attraction, $r_{Min} = \sigma 2^{-1/n}$, mimics the effective cross-linking by linker proteins between elements in the cytoskeleton. By choosing $n = 18$ we get an adhesive soft-sphere potential with $r_{Min} \ll \sigma$ as often used to describe biomolecular assemblies [12, 14]. Finally, motors apply a force \mathbf{f}_i^M on each particle following a stochastic process that mimics the realistic chemical process. For simplicity, we use here a time series of isotropic kicks.

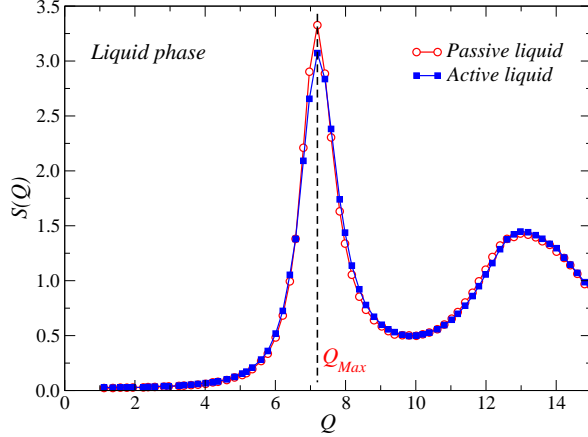


FIG. 1: (Colour online) The static structure factor, $S(Q)$, for a system in equilibrium and driven out of equilibrium by motors with $f^M = 50\%\overline{F}$.

During τ steps of the molecular dynamics trajectory independent forces are applied to a fraction of randomly chosen particles. The strength of the force exerted on each particle is chosen to be a fraction of the mean mechanical force acting on the equivalent passive system, $\overline{F} = \frac{1}{N} \sum_{j=1}^N |\mathbf{f}_{ij}|$. Two types of motors are considered: *adamant* and *susceptible* [12]. The former act in such a way that the direction of the force is chosen at random isotropically: their action is independent of the structural rearrangements they induce. The subset of propelled particles and the directions of the applied forces change at each power stroke of duration τ . Susceptible motors slow down when they drive the system uphill in the (free)-energy landscape. In both cases motors are permanently applied. We neglect hydrodynamic effects.

We integrated Eqs. (1) numerically using Ermak's algorithm [15, 16]. We henceforth use standard Lennard-Jones units: length, energy and time-units are σ , ϵ and $(m\sigma^2/\epsilon)^{\frac{1}{2}}$, respectively [16]. In all our simulations we used 100 independent configurations with 500 particles.

The passive system (motors switched off) is well characterized and presents gas, liquid and crystalline phases depending on the bath temperature and particle density [13]. By tuning the intensity and direction of the non-conservative forces we drive the system near equilibrium (weak perturbation) or far from equilibrium (strong perturbation). We delay the description of the dynamic phase diagram to a more detailed publication. Here we focus on the driven dynamics of a system at conditions such that it is a liquid in equilibrium: $T = 0.8$ and $\rho = 1$.

Let us first discuss the effect of adamant motors. We show data using a time-scale for the power strikes $\tau = 5 \times 10^3$, we apply the force to 10% of the particles and the strength of the non-conservative force, f^M , is indicated in each figure. We start by comparing the

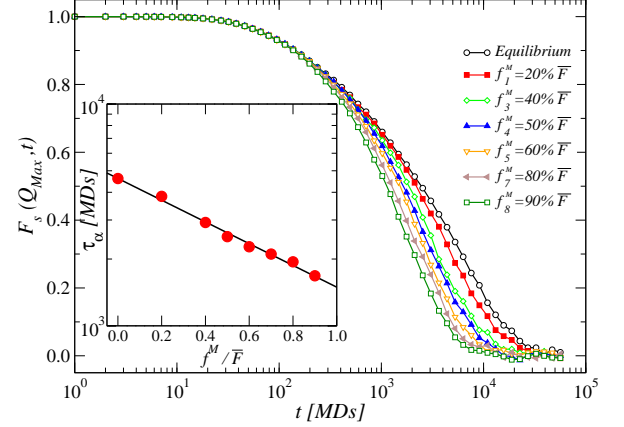


FIG. 2: (Colour online) Main panel: the incoherent intermediate scattering function at $Q = Q_{Max}$, for motor force intensities given in the key. Inset: the dependence of the α relaxation time on the strength of the motor forces with an exponential fit $\tau_\alpha \sim A \exp(-(f^M/f^0))$ with $f^0 \simeq 0.90$.

structure of active and passive matter. In both cases the structure factor, $S(\vec{Q}) = \langle \rho(\vec{Q}, t) \rho^*(\vec{Q}, t) \rangle$, with $\rho(\vec{Q}, t) = N^{-1} \sum_{i=1}^N e^{i\vec{Q}\cdot\vec{r}_i(t)}$ the Fourier transform of the instantaneous density, becomes stationary and isotropic after a short transient: $S(\vec{Q}, t) \rightarrow S(Q)$. In Fig. 1 we show that $S(Q)$ for the passive liquid and the active system with $f^M = 50\%\overline{F}$ are practically identical, with a maximum located at $Q_{Max} \sim 7.1$ in both cases.

The relaxational dynamics of super-cooled liquids and glasses is usually examined by monitoring the decay of the – possibly two-time dependent – incoherent (one-particle) intermediate scattering function $F_s(\vec{Q}, t, t_w) = N^{-1} \sum_{i=1}^N \langle e^{-i\vec{Q}[\vec{r}_i(t+t_w) - \vec{r}_i(t_w)]} \rangle$ [6] with t_w the waiting-time measured after preparation and t the delay time between the total and the waiting times. In the liquid and under the effect of the motors the systems reach an isotropic stationary regime: F_s only depends on Q and t . Figure 2 displays F_s as a function of time-delay in a log-linear scale for several force strengths ranging from zero (equilibrium limit) to 90% \overline{F} . The decay is faster for increasing force strengths though remains relatively slow for all drives as demonstrated by the fact that F_s decays to zero in a logarithmic time-scale. In the inset we show how the α -relaxation time, $\tau_\alpha \equiv F_s(Q, \tau_\alpha) = e^{-1}$, decreases for increasing force strength in a linear-log scale, similarly to the shear-thinning phenomenon. The line is $\tau_\alpha \sim A \exp(-(f^M/f^0))$. At each applied force we find $\tau_\alpha \propto Q^{-2}$ (not shown).

The equilibrium fluctuation-dissipation theorem (FDT) states that the spontaneous fluctuations are related to their associated induced fluctuations by a model-independent formula $T\chi(t, t_w) = C(t=0, t_w) - C(t, t_w)$. C is the connected correlation of two observables O_1 and O_2 , measured at times $t + t_w$ and t_w respectively. χ is

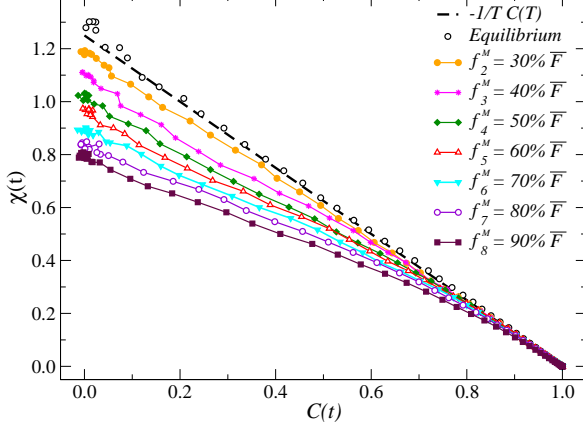


FIG. 3: (Colour online) Parametric representation of the fluctuation-dissipation relation for passive and active matter. The strength of the applied forces are given in the key.

the linear response of the average of the observable O_1 measured at time $t + t_w$ to an infinitesimal perturbation that modifies the Hamiltonian as $H \rightarrow H - hO_2$ from t_w to t : $\chi(t, t_w) = \langle O_1^h(t + t_w) - O_1(t + t_w) \rangle / h$. In interacting particle problems [8] it is customary to use $O_1(t_w) = \frac{1}{N} \sum_{i=1}^N \epsilon_i e^{i\vec{Q}\vec{r}_i(t_w)}$, $O_2(t_w) = 2 \sum_{i=1}^N \epsilon_i \cos[\vec{Q}\vec{r}_i(t_w)]$, with the field $\epsilon_i = \pm 1$ with probability a half. For each system configuration we averaged over 100 field realizations. In Fig. 3 we show the fluctuation-dissipation relation for passive and active matter. The plots are parametric constructions of the integrated linear response χ as a function of the correlation function using t as the parameter [3]. In the equilibrium case, FDT holds and minus the inverse slope of $\chi(C)$ is the temperature of the thermal bath, $T = 0.8$ in this case. In general, all curves join at $(C = 1, \chi = 0)$, as imposed by normalization at $t = 0$. The ‘initial’ slope is determined by the equilibrium FDT [17]. At longer time-differences the curves progressively depart from the equilibrium result to reach other straight lines characterised by slopes that depend on the strength of the motor forces. A time (or correlation) dependent effective temperature is then defined as [3]

$$T_{eff}(C) = -d\chi(C)/dC. \quad (2)$$

Interestingly enough, soon after departure from the equilibrium form, the curves approach a new straight line from which one extracts a single value of the effective temperature – within numerical accuracy [18].

The meaning of T_{eff} as a temperature depends on it verifying a number of conditions expected from such thermodynamic concept. In particular, a temperature should be measurable with a thermometer. A tracer particle with a long internal time-scale (proportional to the square root of its mass) [3, 4, 8] acts as a thermometer that couples to the long time-delay structural rearrange-

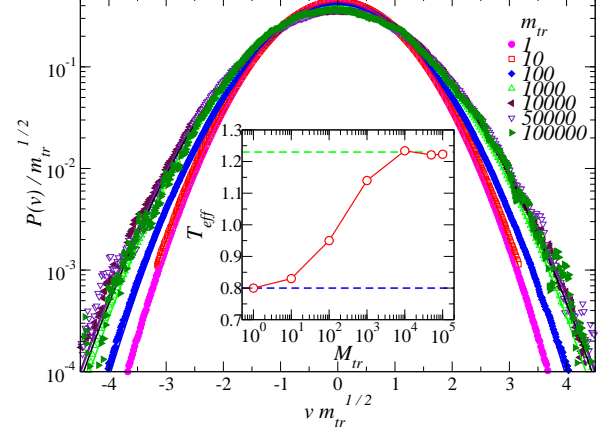


FIG. 4: (Colour online) Main panel: probability distribution function of the velocity v of different tracers with masses m_{tr} given in the key. The motor force intensity is $f^M = 60\%F$. The full lines are fits to the Gaussian form (3). Inset: T_{eff} as function of m_{tr} as obtained from the Gaussian fits to the data-points in the main panel.

ments (and not to the fast vibrations, $t \sim 0$, that yield the ambient temperature, see Fig. 3 and [17]). We then coupled a tracer particle with mass m_{tr} to the active matter *via* the same Lennard-Jones potential, so that we do not modify the structure factor of the fluid. (The tracer does not couple to the thermal bath.) In Fig. 4 we show the tracers’ velocity distributions (for 10 independent tracers). The data points are superposed to

$$P(v) = \sqrt{\frac{m_{tr}}{2\pi T_{eff}}} \exp\left(-\frac{m_{tr}v^2}{2T_{eff}}\right), \quad (3)$$

with T_{eff} the only fitting parameter. The reason why a Maxwellian distribution applies is that the tracer behaves as a normal system immersed in an environment made of active matter. The inset in Fig. 4 displays the dependence of T_{eff} on m_{tr} for one value of the energy pumping force. A very light tracer basically follows the very fast – high frequency – dynamics of its environment and thus measures the bath temperature (lower horizontal dashed line). A heavier tracer feels the slower – low frequency – structural relaxation and measures a higher temperature. A sufficiently heavy tracer only follows the slow dynamics of the sample and therefore measures the actual effective temperature (upper horizontal dashed line), $T_{eff}(f^M = 60\%F) \sim 1.23$.

Finally, in Fig. 5 we compare the values of T_{eff} derived from Eqs. (2) and (3). The two measurements yield consistent results, with T_{eff} increasing from T at zero pump to about $2T$ when the strength of the driving forces equals the one of the mechanical forces. We also found that T_{eff} decreases with decreasing τ (not shown).

Susceptible motors [12] act differently: they slow down when driving the system uphill in the (free)-energy land-

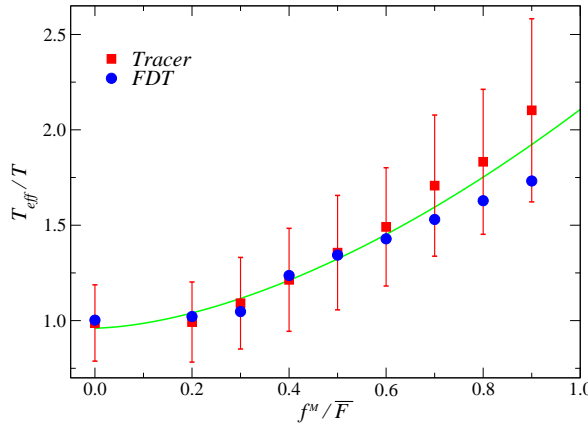


FIG. 5: (Colour online) Effective temperature obtained from response-correlation and massive tracer calculations for different motor force intensities.

scape. It is natural to expect that the effective temperature of such active matter would be *lower* than the one of the thermal bath. We tested the effect of a very simple-minded realization of these motors. For τ time steps the motors attempt to act on a percentage of the particles. Their effect is accepted only if the move leads to a decrease in potential energy. Otherwise, the effect of the motors is neglected and free-relaxation takes place, followed by a new attempt to drive the system. It is clear that the number of accepted moves under the effect of such motors decreases with time and, in practice, the system is not sufficiently driven out of equilibrium. Figure 6 shows a tiny effect, $T_{eff} \lesssim T$. A more detailed study of susceptible motors will be presented elsewhere.

Summarizing, we showed that the notion of an effective temperature, defined by studying the deviations from the equilibrium FDT out of equilibrium can be applied to ac-

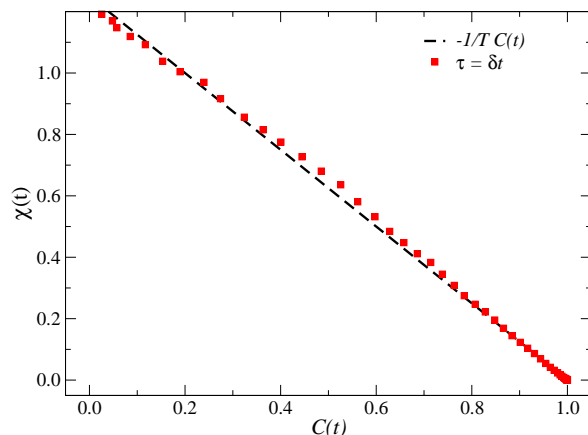


FIG. 6: (Colour online) The parametric plot of linear response against correlation for active matter under the effect of susceptible motors.

tive matter. We demonstrated that the value of the effective temperature measured with a thermometer realized by a tracer particle coincides – within numerical accuracy – with the one obtained from the fluctuation-dissipation relation for all values of the pumping forces. For adamant motors T_{eff} is larger or equal than the bath temperature and increases as a function of the pumping force. This finding is consistent with the intuitive idea that ascribes T_{eff} to the degree of additional agitation caused by the non-conservative forces. Susceptible motors have a very weak effect in driving the system out of equilibrium. For intermediate time-delays the fluctuation-dissipation relation indicates $T_{eff} \lesssim T$ but a much more detailed study is necessary to grasp the dependence on the intervening parameters such as the time-delay between kicks, the strength of the perturbing force, *etc.* in this case. Finally, it is a challenge to derive this results with hydrodynamic theories of the kind proposed in [19].

LFC is a member of Institut Universitaire de France.

- [1] B. Alberts, *The molecular biology of the cell* (Garland, New York, 1994).
- [2] H. C. Berg, *Nature* **254**, 389 (1975); E. Ben-Jacob *et al*, *Phys. Rev. Lett.* **75**, 2899 (1995).
- [3] L. F. Cugliandolo, J. Kurchan and L. Peliti, *Phys. Rev. E* **55**, 3898 (1997); L. F. Cugliandolo and J. Kurchan, *Physica A* **263**, 242 (1999).
- [4] H. Makse and J. Kurchan, *Nature* **415**, 614 (2002).
- [5] F. Zamponi *et al*, *J. Stat. Mech.* (2005) P09013.
- [6] K. Binder and W. Kob, *Glassy materials and disordered solids* (World Scientific, 2005).
- [7] see, *e.g.* P. Wang, C. Song, and H. A. Makse, *Nature Physics* **2**, 526 (2006) and refs. therein.
- [8] L. Berthier and J-L Barrat, *Phys. Rev. Lett.* **89**, 95702 (2002); *J. Chem. Phys.* **116**, 6228 (2002).
- [9] A. B. Kolton *et al*, *Phys. Rev. Lett.* **89**, 227001 (2002).
- [10] T. Lu *et al*, *Biophys. J.* **91**, 84 (2006).
- [11] P. Martin *et al*, *Proc. Nac. Acad. Sc. USA* **98**, 14380 (2001).
- [12] T. Shen and P. G. Wolynes, *Proc. Nac. Acad. Sc. USA* **101**, 8547 (2004); *Phys. Rev. E* **72**, 041927 (2005).
- [13] G. A. Vliegenthart *et al*, *Physica A* **263**, 378 (1999).
- [14] D. F. Rosenbaum and C. F. Zukoski, *J. Cryst. Growth* **160**, 752 (1996).
- [15] D. L. Ermak and J. A. McCammon, *J. Chem. Phys.* **69**, 1352, 1978.
- [16] M. P. Allen and D. J. Tildesley, *Computer simulation of liquids* (Clarendon Press, 2nd ed., 1989).
- [17] L. F. Cugliandolo *et al*, *Phys. Rev. Lett.* **79**, 2168 (1997).
- [18] For a discussion on the separation of time-scales see L. F. Cugliandolo, in *Slow relaxation in glassy systems*, J-L Barrat *et al* eds. (Springer, Berlin, 2003), cond-mat/0210312.
- [19] H. Y. Lee and M. Kardar, *Phys. Rev. E* **64**, 056113 (2001); Y. Hatwalne *et al*, *Phys. Rev. Lett.* **92**, 118101 (2004); T. B. Liverpool and M. C. Marchetti, *Phys. Rev. Lett.* **97**, 268101 (2006); K. Kruse *et al*, *Phys. Rev. Lett.* **92**, 078101 (2004);